Headform Friction Coefficients Relevant to Helmet Testing

Nicole E.-P. Stark, Taylor C. Geiman, Susanna Gagliardi, Matthew Wood, Luca Viano, Steve Rowson

Abstract

The head and helmet frictional interface can affect the head's impact response. However, headforms have known limitations to their biofidelity, including their friction characteristics. This study quantified friction coefficients for the EN960, Hybrid III, and NOCSAE headforms across multiple materials using a specially designed tribometer. We also compared friction coefficients between new and used samples of each headform and measured the effect of friction-reducing skull caps. The static friction coefficients for each headform against high-density foam were 0.29 ± 0.01 for the EN960, 0.97 ± 0.17 for the Hybrid III, and 1.16 ± 0.06 for the NOCSAE and the static friction coefficients against a helmet lining material were 0.48 ± 0.04 for the EN960, 0.83 ± 0.03 for the Hybrid III, and 0.99 ± 0.10 for the NOCSAE [mean ± standard deviation (SD)]. The headforms with COFs closest to that of a human were the EN960 0.29 ± 0.01, NOCSAE with a skull cap 0.29 ± 0.02, and Hybrid III with a skull cap 0.29 ± 0.02. These findings highlight the differences in friction between headforms and that of the human head, allowing for a basis of understanding that can lead to the development of more biofidelic headforms and helmet testing standards.

Keywords headform, friction, helmets

I. INTRODUCTION

The ability of helmets to reduce head injury risk is evaluated through impact testing using dummy headforms. However, various standards and independent test methods use different headforms, including the EN960, Hybrid III, and NOCSAE headforms. These headforms have known limitations to their biofidelity, including their friction characteristics [1-5]. Each headform has a different outer material composition resulting in different frictional interfaces between the headform and helmet. The EN960 headform does not include a skin layer and is entirely comprised of magnesium [6-8]. Unlike the EN960, the Hybrid III and NOCSAE headforms have outer layers to mimic skin. The Hybrid III headform has a vinyl plastisol skin [3,4], and the NOCSAE headform has a polyurethane skin [2,9,10]. The different material designs affect the frictional interface between the headforms and helmets. Several studies, including those by Ebrahim et al. and Trotta et al., have demonstrated that the frictional interaction between the helmet and the head may affect the rotational impact responses and computation of injury criteria [1,6-8,11-14]. This is a crucial aspect to consider because rotational impact response is a dominant predictor of brain injury [15-19].

Multiple studies have evaluated the frictional characteristics of the Hybrid III and EN960 headforms [1,6-8,13,14]. The Hybrid III headform reported coefficient of friction (COF) values to range from 0.75 to 1.07 [7,13]. Due to concerns that these values are too high, some test methods cover the Hybrid III headform with a stocking or skull cap to reduce friction [7,20,21]. Bonin et al. reported a COF of 0.26 when the Hybrid III was equipped with a skull cap and a COF of 0.17 when it wore a wig [13]. Magnesium headforms have a lower friction coefficient with reported COF values ranging from 0.16-0.23 [6-8]. Although the NOCSAE headform is widely employed for helmet testing [9], no documented friction coefficients exist. Even though friction coefficients for the EN960 and Hybrid III headforms have been previously investigated, varying experimental methods with different materials make comparisons between headforms and the human head difficult.

N. E.-P. Stark is a Ph.D. student in Biomedical Engineering (email:nestark@vt.edu phone:410-703-4523), and T. C. Geiman, S. Gagliardi, and M. Wood are undergraduate students in Biomedical Engineering at Virginia Tech in Blacksburg, VA, L. Viano is employed at KASK S.p.A. ad Unico, and S. Rowson is a Professor of Biomedical Engineering and Mechanics at Virginia Tech in Blacksburg, VA.

Trotta et al. measured the COFs of magnesium and Hybrid III headforms against a helmet lining material and directly compared them to the human head [7]. They concluded that both headforms were significantly different from the human head. However, human head COFs were measured on cadaveric samples and did not account for the power-law relationship between normal force and friction. COF comparisons between dummy and human heads must be made at matched normal forces because COFs will decrease with increasing normal force [22]. Another concern that previous work has yet to examine is how the frictional characteristics of headforms change over time. Polyurethane and vinyl plastisol oxidise and degrade over time, and many headforms undergo repetitive impacts resulting in wear markings [23,24].

Standardizing headform frictional properties has the potential to enhance the biofidelity of impact responses during helmet testing and can provide information to optimise helmet designs. This study's objectives were to (1) quantify the EN960, Hybrid III, and NOCSAE headforms' COFs, (2) compare COF across headforms and against multiple materials, (3) quantify the effect of adding friction-reducing skull caps to the headforms, and (4) compare headform COFs to that of a human at matched normal forces. These findings will directly apply to optimizing headform biofidelity, refining helmet testing protocols, and defining frictional boundary conditions for computational models.

II. METHODS

Tribometer Design and Validation

We developed a custom tribometer to measure the COFs of different headforms against multiple materials. The device consists of a headform mount, a sled, and a tension load application (Fig. 1). An inverted headform is secured to a vertically sliding frame using custom headform mounts. This configuration allows for normal force on the sled to be controlled by adding weights to the top of the headform mount.

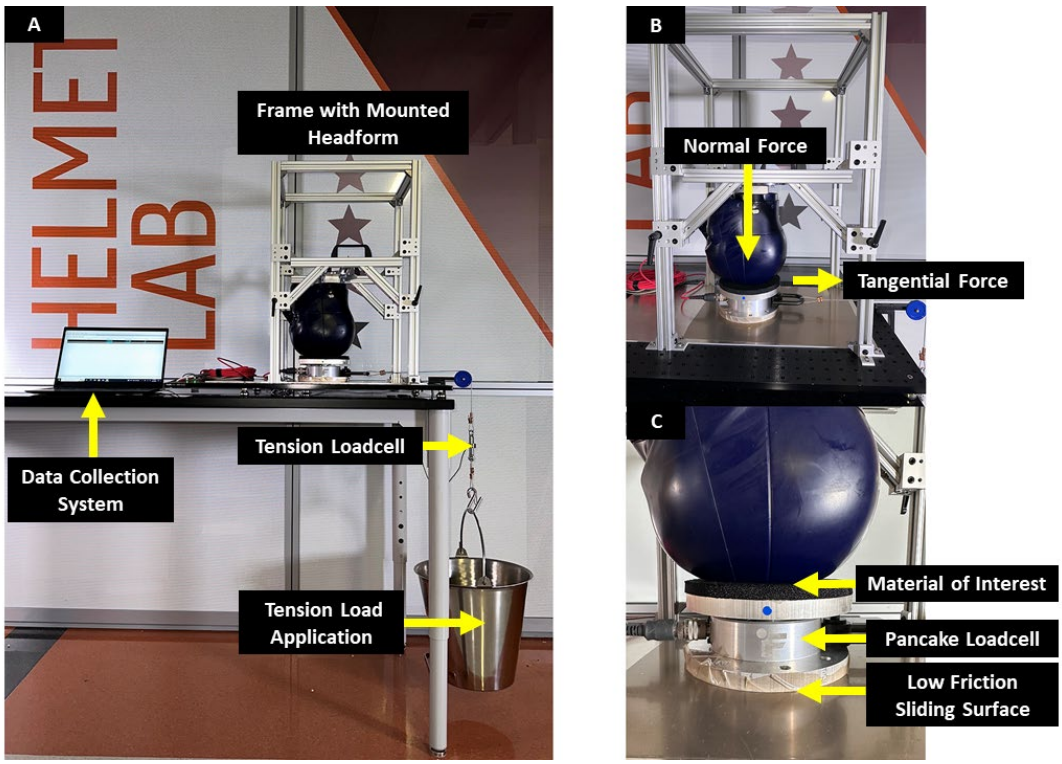

Figure 1: Custom tribometer used to measure the static friction coefficient of the dummy headforms. (A) Total tribometer including the fixed frame, sled, tension load application, and tension load cell. (B) Fixed frame and inverted mounted headform, showing the normal and tangential force. (C) The sled containing the materials being tested, a pancake load cell to measure the normal force application, and a low-friction sliding surface.

The sled consists of a pancake load cell (LCF 450 Low Profile Universal Pancake, Resolution 0.4 N, FUTEK Irvine, CA) placed between the material of interest and the low friction sliding surface (Fig. 1). The pancake load cell measures the normal force applied by the mounted headform to the material begin tested. After reaching the target normal force, a bucket is attached to the sled with a steel cable laid over a pulley off the table's edge. The tangential force is incrementally increased by adding 0.20 g to a bucket until movement is generated. This applied tangential force was measured and recorded using an in-line tension load cell (LCM300 Tension and Compression Loadcell Resolution 0.4 N, FUTEK Irvine, CA).

The sled experiences two frictional forces; the first is between the material of interest and the mounted headform, and the second is the friction of the system which is between the Teflon-covered bottom of the sled and the Teflon-covered base plate. This assumes the pulley is frictionless. Before, during, and after a test configuration, we measured the COF of the system at a matched normal force to the headform test three times. We then used the friction of the system when computing the COF of the headform on each material of interest (Eq. 1). *Derivation can be found in Appendix A.*

$$\mu_{headform} = \frac{T - \mu_{system}(F_H + m_{sled} * g) - m_{sled} * (g - T/m_{bucket})}{F_H} \quad \text{Eq. 1}$$

where T is the tangential force from the tension in the cable (N), μ_{system} is the average static COF of the bottom of the sled and the base over three trials, m_{sled} is the mass of the sled (kg), F_H is the normal force measured by the pancake loadcell applied by the headform (N), and m_{bucket} is the ending mass of the bucket (kg).

The static COF occurs just before movement of the sled occurs and therefore the acceleration is zero, reducing the COF equation (Eq 2).

$$Static\ \mu_{headform} = \frac{T - \mu_{system}(F_H + m_{sled} * g)}{F_H} \quad \text{Eq. 2}$$

The duration of impact events is typically between 5-15 milliseconds, and the static COF plays a dominant role in determining the response due to the rapid nature of the event. Furthermore, prior research has indicated that, when it comes to helmeted applications, the difference in human head static and dynamic COFs can be disregarded [22]. As a result, this study concentrates on examining the static COF of headforms and headform alterations.

To validate our tribometer, we compared five static friction coefficients of different materials collected using a classic angle-based inclined plane friction measurement and the custom tribometer device [25]. Materials tested included polyester, Teflon, helmet liner used in a KASK Protone Icon, aluminum, polylactic acid, and wood, all against aluminum. We performed a Bland-Altman analysis to determine the mean bias between systems [26]. A paired t-test and 95% limits of agreement were used to evaluate the difference in the two measurement techniques, with a significance level of 0.05 [27].

Experimental Testing

We quantified headform static friction coefficients against multiple materials using our tribometer (Table 1). These materials included EPP high-density foam (50 kg/m^3), a helmet liner material (from a KASK Protone Icon), Teflon, aluminum, and polyester fabric. To evaluate the effects of degradation and oxidation, we tested new and laboratory-used NOCSAE, Hybrid III, and EN960 headforms. The used NOCSAE headform that was 5 years old, while the Hybird III headform was 3 years old, and EN960 headform was 13 years old. Each used headform has been used regularly for conducting impact tests and have noticeable wear. Based on previous research, we anticipated that the Hybrid III and NOCSAE headforms would produce COFs much higher than what has been measured from humans [7,13]. For this reason, we examined the effects of adding skull caps (NIKE PRO Skull Cap 2.0) to the Hybrid III and NOCSAE headforms [7,20,21]. We conducted five trials for each headform and material condition. We also conducted three system COF measurements during the five trials after the first, third, and fifth trials. These trials consisted of loading the sled to a matched normal force using free weights, then performing a collection. This allowed us to quantify the COF of the low-friction base. The equations and assumptions used to calculate the COF of the system are derived in Appendix A.

Table 1: Factor levels for static COF testing

Headform	Material	Condition	Modification
NOCSAE	Foam	New	Skull Cap
Hybrid III	Helmet Liner	Used	None
EN960	Polyester		
	Teflon		
	Aluminum		

Each headform was securely mounted, leveled, and weighted to apply an 80 N normal force to the tested material. An 80 N normal force was used as it is within the range of normal forces previously used to capture human head COF and for direct comparison to defined human head static COF at 80 N [6,7,22]. The normal force was measured using the sled-mounted pancake load cell for each test. The tangential force was then incrementally increased through tension in the cable by adding 0.20 g to a bucket until movement was generated. Data were collected at 400 Hz from both the pancake and in-line tension load cells. Force signals were filtered using a 4-pole phaseless lowpass Butterworth filter with a 17 Hz cut-off frequency. Force signals were then smoothed using a 50 ms moving average window. The COF over time was calculated for each trial (Eq. 1) and the static COF was quantified. The static COF was defined as the peak COF right before movement occurred, after which COF either leveled off or decreased. The dynamic COF was defined as the average of the plateau during movement.

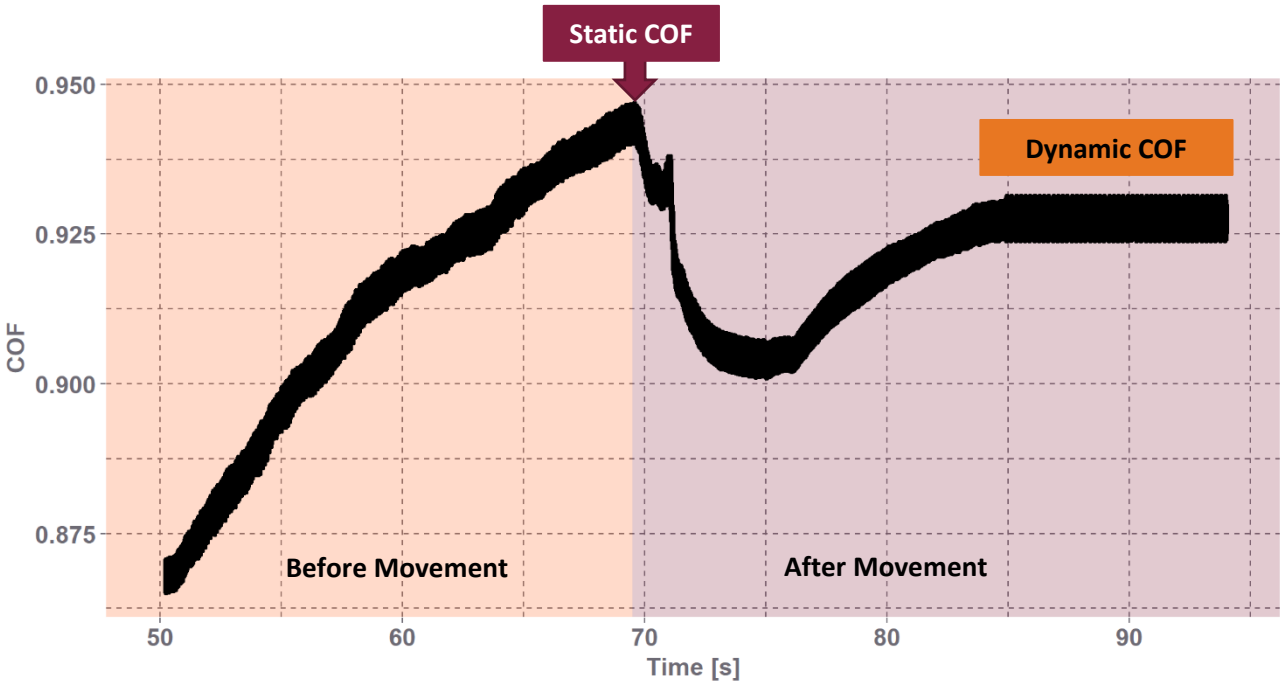

Figure 2: The calculated COF over time for a single trial. The shaded orange region is the start of applied force before movement occurs, and the shaded red region is the start of sled movement after overcoming the static COF. The static COF was defined as the peak COF before movement occurred and the dynamic COF was defined as the average of the plateau during movement.

Statistical Analysis

The differences in static COF between headform, condition, material, and modification were evaluated using an ANOVA and post hoc Tukey honestly significant difference (HSD) test. The Tukey HSD test adjusted the p-values for multiple comparisons using the Tukey-Kramer method. We also computed the mean difference (Δ) with a 95% confidence interval (CI). All statistical analyses were performed using R (2022.12.0), and the significance threshold was set to 0.05.

III. RESULTS

Tribometer Validation

There were no differences in measured static COF between our headform tribometer and the angle-based devices across all materials (Table 2). When comparing our tribometer device with the angle-based device, we found a mean bias of 0.00 with a 95% limit of agreement of -0.01 to 0.02. The upper and lower limits of agreement represent the range within which 95% of differences between the two measurement methods are expected to lie.

Table 2: The static COF [mean ± SD] measured by an angle-based inclined plane friction device and our headform tribometer device and the paired t-test showed no difference in measurement technique. The mean bias and 95% limits of agreement were calculated based on a Bland-Altman analysis.

Material Against Aluminum	Angle-Based Static COF	Our Tribometer Static COF	p-value
Polylactic Acid	0.23 ± 0.02	0.23 ± 0.06	0.92
Wood	0.22 ± 0.01	0.21 ± 0.08	0.80
Aluminum	0.21 ± 0.00	0.22 ± 0.04	0.72
Teflon	0.09 ± 0.01	0.09 ± 0.05	0.99
Polyester	0.23 ± 0.01	0.22 ± 0.11	0.88
Helmet Liner	0.23 ± 0.01	0.22 ± 0.02	0.37

Mean bias 0.00 and 95% limit of agreement -0.01 to 0.02

Headform Testing

For new and unused headforms, we measured the static COF of the EN960 as 0.29 ± 0.01, the Hybrid III as 0.97 ± 0.11, and the NOCSAE as 1.16 ± 0.06 against high-density foam. Against the helmet lining material, the static COFs were 0.48 ± 0.04 for the EN960, 0.83 ± 0.03 for the Hybrid III, and 1.00 ± 0.10 for the NOCSAE. Headform model significantly influenced static COF ($p < 0.001$). The NOCSAE and Hybrid III headforms COFs were significantly different ($p < 0.001$), but the difference was small ($\Delta = -0.07$, 95% CI = [-0.11 to -0.04]). However, the EN960 had significantly lower COF ($p < 0.001$) than both the NOCSAE ($\Delta = 0.54$, 95% CI = [0.50 to 0.57]) and the Hybrid III ($\Delta = 0.61$, 95% CI = [0.58 to 0.65]). The material also affected COF ($p < 0.001$). Moreover, the COF of each headform varied against each material in the following order: Teflon < aluminum < polyester < helmet liner < foam (Fig. 3, Table 3).

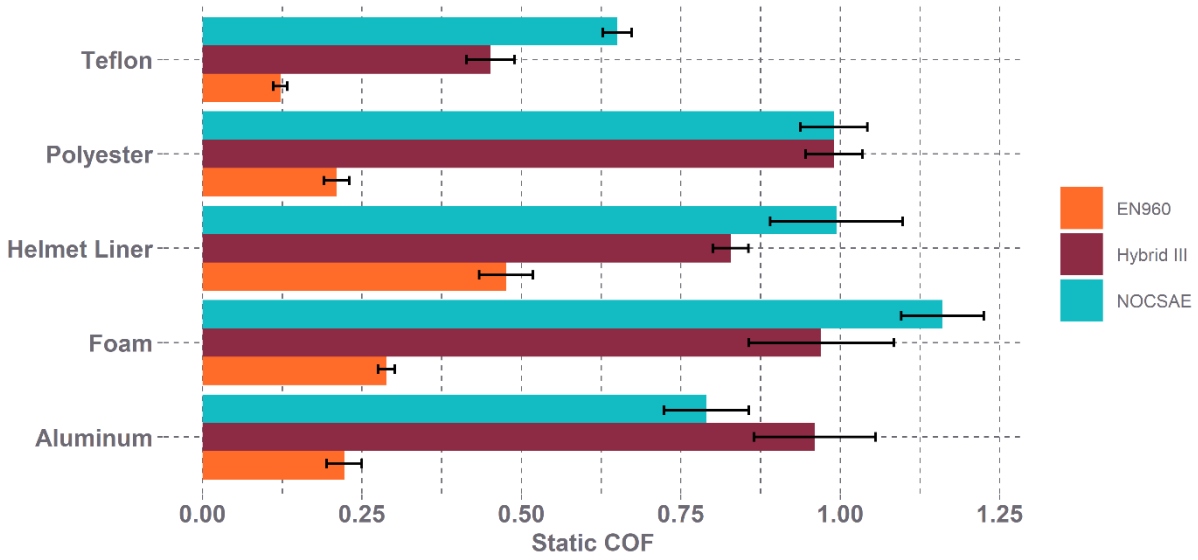

Fig. 3. Static friction coefficients (mean ± SD) for the EN960, Hybrid III, and NOCSAE headforms against multiple materials (Teflon, Polyester, Helmet Liner, High-Density Foam, Aluminum). The NOCSAE and Hybrid III have similar friction coefficients, while the EN960 has lower friction coefficients.

Headform condition influenced COF ($p < 0.001$). The used headforms COFs against foam were 0.92 ± 0.04 for the NOCSAE, 1.20 ± 0.02 for the Hybrid III, and 0.31 ± 0.03 for the EN960. Against a helmet liner, the static COF was 0.83 ± 0.05 for the NOCSAE, 0.91 ± 0.04 for the Hybrid III, and 0.34 ± 0.02 for the EN960 (Fig. 4). Differences between new and used headforms was not significant for the EN960 ($p = 0.43$, $\Delta = -0.05$, 95% CI = [-0.12 to -0.02]), but were for the NOCSAE ($p < 0.001$, $\Delta = -0.19$, 95% CI = [-0.25 to -0.13]) and Hybrid III ($p < 0.001$, $\Delta = 0.11$, 95% CI = [0.05 to -0.16]) headforms.

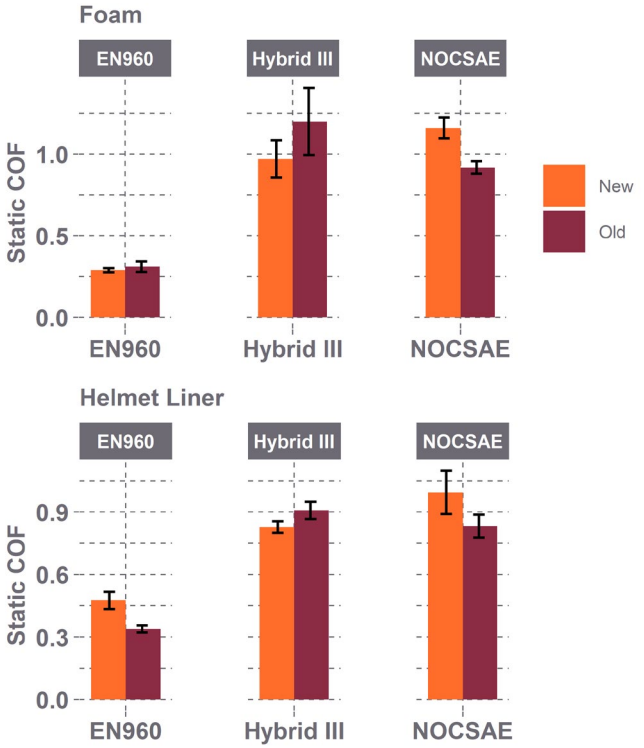

Fig. 4. Static coefficient of friction (COF) mean ± SD comparing the condition of EN960, Hybrid III, and NOCSAE headforms against high-density foam and helmet liner material. Used condition decreased NOCSAE COF and increased Hybrid III COF.

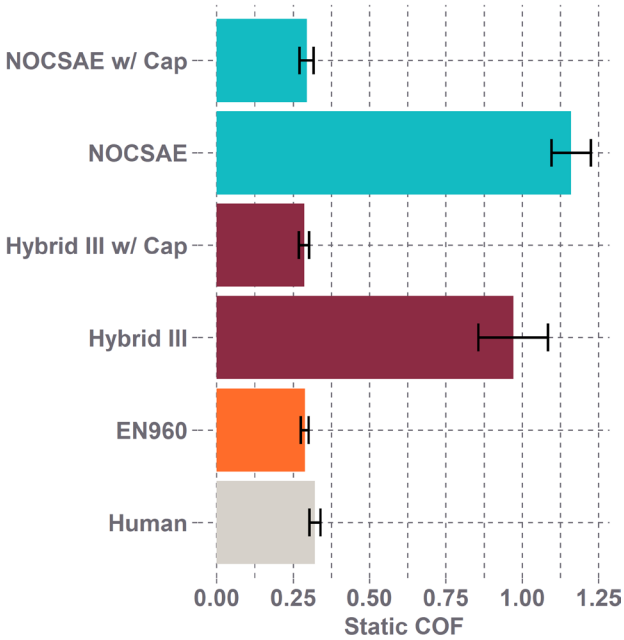

Fig. 5. Human head and different headforms static coefficient of friction (COF) mean ± SD CIs against high-density foam. Adding a skull cap reduced the COF of the NOCSAE and Hybrid III headform, similar to the COF of the EN960 and the human head.

The addition of a skull cap significantly reduced the static COF of both the NOCSAE ($p < 0.001$, $\Delta = -0.51$, 95% CI = [-0.56 to -0.46]) and Hybrid III ($p < 0.001$, $\Delta = -0.58$, 95% CI = [-0.63 to -0.53]) headforms against foam and the helmet liner material (Fig. 5, Table 3).

Table 3: Static coefficient of friction (COF) [mean ± SD] for each headform, headform modifications tested, and published human head values.

Material	NOCSAE	Hybrid III	EN960	NOCSAE + Skull Cap	Hybrid III + Skull Cap	Human Head
Foam	1.16 ± 0.06	0.97 ± 0.11	0.29 ± 0.01	0.29 ±0.02	0.29 ± 0.02	0.30-0.34[22]
Helmet Liner	0.99 ± 0.10	0.83 ± 0.03	0.48 ± 0.04	0.38 ±0.02	0.37 ± 0.02	-
Teflon	0.65 ± 0.02	0.45 ± 0.04	0.12 ± 0.01	-	-	-
Polyester	0.99 ± 0.05	0.99 ± 0.04	0.21 ± 0.01	-	-	0.21-0.35[7]
Aluminum	0.79 ± 0.06	0.96 ± 0.10	0.22 ± 0.02	-	-	-

The dynamic COF did not differ from the static COF (Table 4).

Table 4: Dynamic coefficient of friction (COF) [mean ± SD] for each headform, headform modifications tested, and published human head values.

Material	NOCSAE	Hybrid III	EN960
Foam	1.15 ± 0.03	0.97 ± 0.10	0.29 ± 0.01
Helmet Liner	1.00 ± 0.03	0.83 ± 0.01	0.48 ± 0.04
Teflon	0.64 ± 0.02	0.47 ± 0.02	0.13 ± 0.01
Polyester	0.99 ± 0.04	1.00 ± 0.02	0.21 ± 0.00
Aluminum	0.75 ± 0.08	1.04± 0.09	0.23 ± 0.03

IV. DISCUSSION

The frictional interface between a headform and helmet has been suggested to affect rotational impact response [1,6-8,11-19]. This study investigated the frictional properties of commonly used dummy headforms in helmet testing. Due to the unique shape of the headforms, a tribometer was designed to measure headform COFs. Validation of our tribometer and COF calculation method found a mean bias of 0.00 compared to an angle-based friction measurement and suggested that 95% of all measurements will be between -0.01 and 0.02 of the incline plane's measurement. Our method allowed us to quantify COF for the different interface conditions we investigated reliably. The headform tribometer also exhibits comparable sensitivity to commercially available tribometers, which typically offer a sensitivity of 0.002 - 0.04 [28-30].

In this study, we identified that the static COF varied between headform models, condition of the headforms, modification, and material tested against. Though the NOCSAE headform is used across standards and lab protocols [2,9,10], previous studies have yet to quantify the NOCSAE headform's COF. We quantified the NOCSAE COF and found it similar to the Hybrid III. Previous studies reported a friction coefficient of 0.75 ± 0.06 and 1.07 for the Hybrid III headform against a polyester material [7,12,13]. We report a friction coefficient within the range of previous work (0.99 ± 0.05). The EN960 headform's COF has previously been reported as 0.16 ± 0.03 and 0.20 against polyester [7,8], and we found a similar COF of 0.20 ± 0.02 for the EN960 against polyester. Another study found a COF of 0.23 for the EN960 against padding inside an HJC helmet [6]. Although we did not test against similar padding, when compared against high-density foam, another compressive material, we found a higher COF for the EN960 0.30 ± 0.01. The differences between this study's values and those previously published values could be due to differences in the tested polyester materials or applied normal force.

Due to the higher friction of the Hybrid III skin, some test methods cover the Hybrid III headform with a stocking or skull cap to reduce friction [7,20,21]. With skull caps, the static COF of the new NOCSAE headform was decreased by 62% against the helmet liner material and 75% against foam, and the new Hybrid III was reduced by 56% against the helmet liner material and 70% against foam. We also found a similar COF to Bonin et al. when a skull cap was applied to the Hybrid III, 0.26 compared to our 0.29 ± 0.02 [13]. However, to determine the

meaningfulness of reducing the friction coefficient with a skull cap, it is imperative to compare headform friction coefficients to human head friction coefficients.

This study found the material used in helmets can affect the COF of headforms. This is an important factor to consider, especially since many helmets use a poly-blend comfort liner that can have various properties affecting the frictional interface. It's worth noting that the COF results mentioned in this study may only be relevant to the specific liner or polyester material tested. While the study did observe slight differences between the COF of the helmet liner and the polyester tested, it's still unknown how headform COF impacts oblique helmet testing. Therefore, it's unclear whether these minor changes in friction have any significant impact on head impact kinematics. This study also determined that the dynamic COF for each headform was within the SD of static COF. Therefore, for helmeted applications, like the human head, the difference in static and dynamic headform COF can also be disregarded.

In an earlier study, we quantified the human head static COF for 74 participants that slid their heads along EPS foam at varying levels of normal forces (10-150 N) [22]. We found that the static COF of the head against foam decreased with increasing normal force based on a power law relationship. Using this relationship, we defined the 95% CI for the static COF of the human head at 80 N against helmet foam to be 0.30-0.34 [22]. At 80 N, the NOCSAE and Hybrid III had over three times the COF of the human head against foam. However, when covered with a skull cap, the NOCSAE (0.27-0.33) and Hybrid III (0.27-0.31) COF 95% CIs overlapped the human head 95% CI. The EN960's COF 95% CI (0.27-0.30) was also within the human head 95% CI. These results suggest that any headforms can reasonably represent the human head's friction characteristics; however, the Hybrid III and NOCSAE headforms should be equipped with a friction-reducing skull cap to best represent a human head.

This study was limited by only quantifying the COF of each headform and variation at 80 N, but this allowed a direct comparison to the human head's static COF. When considering the relevance of an 80 N normal force, it's important to note that there is a limited amount of force that can be applied to living of cadaver participants when quantifying human head COF. There are ethical concerns regarding the safety of living participants, and high normal force could damage non-living tissue. Overall, this study allows for comparison of COF between different headforms, headform alterations, and human participant results. Moreover, these results can be used to evaluate the influence of COF on the impact event because the headform COF was taken with the same technique and force across all headforms and alterations.

Our results also showed that the degradation and oxidation of the Hybrid III vinyl plastisol and NOCSAE polyurethane affect their static COFs. This was not observed with the EN960. The COF of the Hybrid III increased, which could have resulted from vinyl plastisol becoming tacky with wear. An opposite effect occurred for the COF of the NOCSAE headform. The COF of the NOCSAE headform decreased for the laboratory-used headforms. We believe this was due to the oxidation and hardening of the NOCSAE polyurethane skin. However, this study did not quantify the degradation, oxidation, or amount of use of the used headforms tested. Thus, this study could not draw direct conclusions as to the effects of each of these properties, and this should be considered in the future. Modifying the NOCSAE and Hybrid III headform with a skull cap reduced their COFs to similar levels and using a skull cap for these headforms would reduce concern in headform-to-headform variance over time.

This study was limited by not considering the frictional interface between the skull and scalp. Trotta et al. determined that the scalp affected both linear and rotational acceleration. Still, they did not determine if this result was due to the reduction in friction or the addition of another slip plane [11]. However, our comparative human head data set evaluated the overall human head COF and helmet foam. In this study, it was also assumed that the pulley was frictionless, but its effect is likely negligible. This study's main limitation is that we don't know what effect our reported differences in COF have on head kinematics during helmet testing. The question of how much COF can vary without affecting kinematic response remains. Previous studies have provided mixed results [6,8,14]. Thus, future work should continue to investigate how headform friction affects linear and rotational impact kinematics during oblique impacts.

V. CONCLUSIONS

The EN960, Hybrid III with a skull cap, and NOCSAE with a skull cap produced COFs most similar to values reported for the human head. This study presents a comprehensive analysis of friction coefficients for the EN960, Hybrid III, and NOCSAE headforms across multiple materials, including the condition of the headforms, as well as

with and without skull caps. Adding a skull cap to the NOCSAE and Hybrid III headform may be needed to reduce the effect of COF variance between headforms and changes in condition over time. Standardizing headform frictional properties may be necessary to ensure consistency between test methods and accurate representation of the human head. For now, the effect of headform COF on kinematic response during helmet testing needs further investigation. Ultimately, these results may be used to develop improved headforms, more realistic helmet testing standards, and improved boundary conditions in computation models.

VI. ACKNOWLEDGEMENT

KASK S.p.A. ad Unico socio provided funding support for the completion of this project.

VII. REFERENCES

[1] Aare, M. and Halldin, P. A New Laboratory Rig for Evaluating Helmets Subject to Oblique Impacts. *Traffic Injury Prevention*, 2003. 4(3): p. 240-248

[2] Cobb, B.R., MacAlister, A., et al. Quantitative comparison of Hybrid III and National Operating Committee on Standards for Athletic Equipment headform shape characteristics and implications on football helmet fit. *Proceedings of the Institution of Mechanical Engineers, Part P: Journal of Sports Engineering and Technology*, 2015. 229(1): p. 39-46

[3] Hubbard, R.P. and Mcleod, D.G. Definition and Development of A Crash Dummy Head. *Proceedings of 18th Stapp Car Crash Conference (1974)*, 1974.

[4] Wood, G.W., Panzer, M.B., Bass, C.R., and Myers, B.S. Viscoelastic Properties of Hybrid III Head Skin. *SAE International Journal of Materials and Manufacturing*, 2010. 3(1): p. 186-193

[5] York, S., Edwards, E.D., et al. Influence of Friction at the Head-Helmet Interface on Advanced Combat Helmet (ACH) Blunt Impact Kinematic Performance. *Mil Med*, 2022

[6] Ebrahimi, I., Golnaraghi, F., and Wang, G.G. Factors Influencing the Oblique Impact Test of Motorcycle Helmets. *Traffic Injury Prevention*, 2015. 16(4): p. 404-408

[7] Trotta, A., Ní Annaidh, A., Burek, R.O., Pelgrims, B., and Ivens, J. Evaluation of the head-helmet sliding properties in an impact test. *Journal of Biomechanics*, 2018. 75: p. 28-34

[8] Óscar Juste-Lorente , M.M., Mathieu Piccand, and Francisco J. López-Valdés. The Influence of Headform/Helmet Friction on Head Impact Biomechanics in Oblique Impacts at Different Tangential Velocities. *Applied science*, 2021. 11(11318)

[9] Hodgson, V.R. National Operating Committee on Standards for Athletic Equipment football helmet certification program. *Medicine and Science in Sports*, 1975. 7(3): p. 225-232

[10] Gwin, J.T., Chu, J.J., et al. An investigation of the NOCSAE linear impactor test method based on in vivo measures of head impact acceleration in American football. *J Biomech Eng*, 2010. 132(1): p. 011006

[11] Trotta, A., Zouzias, D., De Bruyne, G., and Ní Annaidh, A. The Importance of the Scalp in Head Impact Kinematics. *Annals of Biomedical Engineering*, 2018. 46(6): p. 831-840

[12] Yu, X., Halldin, P., and Ghajari, M. Oblique impact responses of Hybrid III and a new headform with more biofidelic coefficient of friction and moments of inertia. *Front Bioeng Biotechnol*, 2022. 10: p. 860435

[13] Bonin, S.J., DeMarco, A.L., and Siegmund, G.P. The Effect of MIPS, Headform Condition, and Impact Orientation on Headform Kinematics Across a Range of Impact Speeds During Oblique Bicycle Helmet Impacts. *Ann Biomed Eng*, 2022. 50(7): p. 860-870

[14] Finan, J.D., Nightingale, R.W., and Myers, B.S. The Influence of Reduced Friction on Head Injury Metrics in Helmeted Head Impacts. *Traffic Injury Prevention*, 2008. 9(5): p. 483-488

[15] Kleiven, S. Predictors for traumatic brain injuries evaluated through accident reconstructions. *Stapp Car Crash J*, 2007. 51: p. 81-114

[16] Kleiven, S. Why Most Traumatic Brain Injuries are Not Caused by Linear Acceleration but Skull Fractures are. *Front Bioeng Biotechnol*, 2013. 1: p. 15

[17] Bland, M.L., McNally, C., Zuby, D.S., Mueller, B.C., and Rowson, S. Development of the STAR Evaluation System for Assessing Bicycle Helmet Protective Performance. *Ann Biomed Eng*, 2020. 48(1): p. 47-57

[18] Rowson, S. and Duma, S.M. Brain injury prediction: assessing the combined probability of concussion using linear and rotational head acceleration. *Ann Biomed Eng*, 2013. 41(5): p. 873-82

[19] Rowson, S., Duma, S.M., et al. Rotational Head Kinematics in Football Impacts: an Injury Risk Function for Concussion. *Ann Biomed Eng*, 2012. 40(1): p. 1-13

[20] DiGiacomo, G., Tsai, S., and Bottlang, M. Impact Performance Comparison of Advanced Snow Sport Helmets with Dedicated Rotation-Damping Systems. *Ann Biomed Eng*, 2021. 49(10): p. 2805-2813
[21] Takhounts, E.G., Craig, M.J., Moorhouse, K., McFadden, J., and Hasija, V. Development of Brain Injury Criteria (BrIC). *Proceedings of 57th Stapp Car Crash Conference*, 2013.
[22] Stark, N.E.-P., Clark, C., and Rowson, S. Human Head and Helmet Interface Friction Coefficients with Biological Sex and Hair Property Comparisons. *Ann Biomed Eng* 2023. Submitted
[23] Perito, E.D. Chemical, thermal and mechanical evaluation of poly(vinyl chloride) plastisol with different plasticizers. *Journal of Elastomers & Plastics*, 2022
[24] Christenson, E.M., Anderson, J.M., and Hiltner, A. Oxidative mechanisms of poly(carbonate urethane) and poly(ether urethane) biodegradation: in vivo and in vitro correlations. *J Biomed Mater Res A*, 2004. 70(2): p. 245-55
[25] Kelemenova, T., Dovica, M., et al. Specific Problems in Measurement of Coefficient of Friction Using Variable Incidence Tribometer. *Symmetry-Basel*, 2020. 12(8)
[26] Giavarina, D. Understanding Bland Altman analysis. *Biochem Med (Zagreb)*, 2015. 25(2): p. 141-51
[27] Myles, P.S. and Cui, J. Using the Bland-Altman method to measure agreement with repeated measures. *Br J Anaesth*, 2007. 99(3): p. 309-11
[28] "Coefficient of Friction Tester – QT-COF Series" Internet https://www.worldoftest.com/coefficient-friction-tester-qt-cof-series. 3/10/2023].
[29] "Slide Angle Coefficient of Friction (COF) Tester 32-25" Internet https://industrialphysics.com/product/32-25-slide-angle-coefficient-of-friction-cof-tester/. 3/10/2023].
[30] "COEFFICIENT OF FRICTION TESTER - INCLINE PLANE" Internet https://idminstruments.com.au/testing-instruments/products/coefficient-of-friction-tester-incline-plane.html. 3/10/2023].

VIII. APPENDIX A

Derivation for the COF equation.

$$Static\ \mu_{headform} = \frac{T - \mu_{system} * (m_{sled} * g + F_H)}{F_H} \quad \text{Eq. 2}$$

where T is the tangential force from the cable tension (N), μ_{system} is the average static COF of the system averaged over three trials, m_{sled} is the mass of the sled (kg), F_H is the normal force applied by the head (N), and m_{bucket} is the ending mass of the bucket (kg).

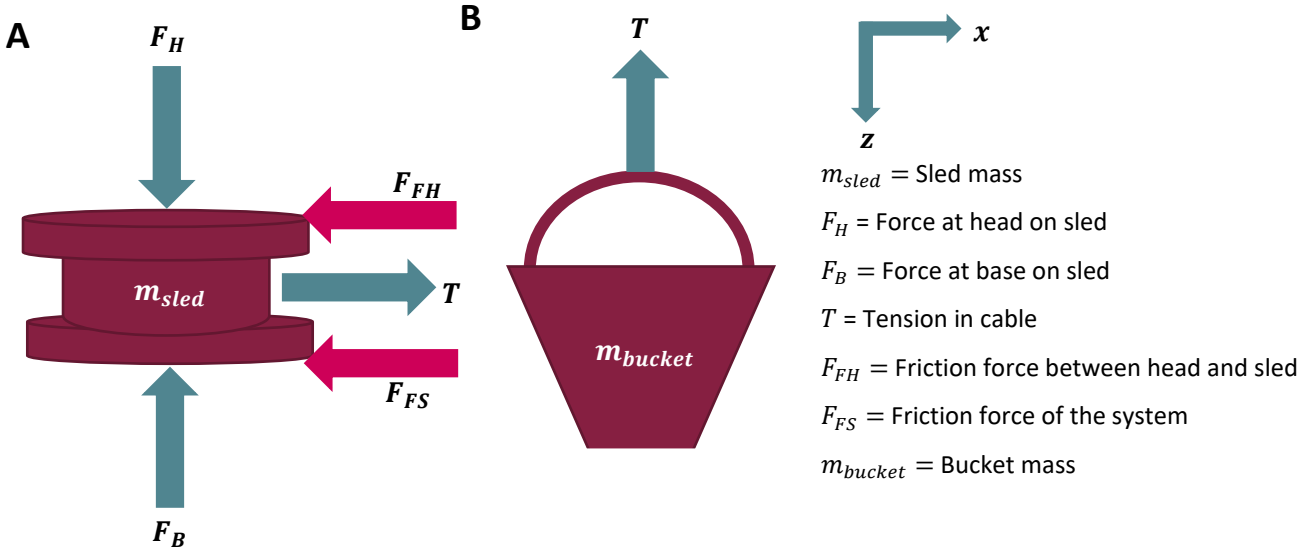

Figure A1: Free body diagrams that was used to calculate the COF of the system. (A) is the free body diagram of the sled. (B) is the free body diagram of the bucket. This assumes the pulley is frictionless. This was used to calculate the COF of each headform to account for the friction of the base and pulley system.

<u>COF of the Headform</u>

Calculation for the bucket to find the acceleration of the system (Fig A1 A), assuming the pulley is frictionless.

$$\sum F_z = m * a$$

$$m_{bucket} * g - T = m_{bucket} * a$$

$$a = g - \frac{T}{m_{bucket}} \quad \text{Eq. A1}$$

Calculation for the sled to find the friction between the headform and the material of interest (Fig A1 A).

$$\sum F_x = m * a$$

$$T - F_{FS} - F_{FH} = m_{sled} * a$$

$$F_{FS} = \mu_{system}(F_H + m_{sled} * g)$$

$$F_{FH} = \mu_{headform} F_H$$

$$T - \mu_{system}(F_H + m_{sled} * g) - \mu_{headform} F_H = m_{sled} * a \quad \text{Eq. A2}$$

Substitute Eq. A1 into Eq A2.

$$T - \mu_{system}(F_H + m_{sled} * g) - \mu_{headform} F_H = m_{sled} * (g - F_T/m_{bucket})$$

$$\mu_{headform} = \frac{T - \mu_{system}(F_H + m_{sled} * g) - m_{sled} * (g - T/m_{bucket})}{F_H} \quad \text{Eq. A3}$$

Static COF occurs just before the movement of the sled and the acceleration is zero. This results in the below equation.

$$Static\ \mu_{headform} = \frac{T - \mu_{system}(F_H + m_{sled} * g)}{F_H} \quad \text{Eq. A4}$$

COF of the System

Calculation for the bucket to find the acceleration of the system (Fig A1 B), assuming the pulley is frictionless.

$$\sum F_z = m * a$$

$$m_{bucket} * g - T = m_{bucket} * a$$

$$a = g - \frac{T}{m_{bucket}} \quad \text{Eq. A5}$$

Calculations for the sled to find the friction of the system (Fig A1 A).

$$\sum F_x = m * a$$

$$T - \mu_{system}(F_H + m_{sled} * g) = m_{sled} * a \quad \text{Eq. A6}$$

Substitute Eq. A5 into Eq A6.

$$T - \mu_{system}(F_H + m_{sled} * g) = m_{sled} * (g - T/m_{bucket})$$

$$\mu_{system} = \frac{T - m_{sled} * (g - T/m_{bucket})}{F_H + m_{sled} * g} \quad \text{Eq. A7}$$

Static COF occurs just before the movement of the sled and the acceleration is zero. This results in the below equation.

$$Static\ \mu_{system} = \frac{T}{F_H + m_{sled} * g} \quad \text{Eq. A8}$$